

STABILITY OF ZrSiN NANOCOMPOSITE FILMS AT AIR ANNEALING

I.A. Saladukhin¹, G. Abadias², V.V. Uglov¹, S.V. Zlotski¹

¹ Dpt. of Solid State Physics, Belarusian State University, 4 Nezavisimosti ave.,
220030 Minsk, BELARUS, solodukhin@bsu.by

² Institut P', Université de Poitiers-CNRS-ENSMA, SP2MI, Téléport 2, F86962 Chasseneuil-Futuroscope, FRANCE, gregory.abadias@univ-poitiers.fr

Introduction Thin films on the basis of nitrides of transitional metals (TM) are widely used as hard protective coatings in the industry. One of the most important properties of the coatings for their practical application is their resistance to high temperature oxidation. For such severe conditions, most of the mononitride films cease to perform their protective function. For example, TiN coatings are rapidly oxidized at temperatures as low as 550 °C /1/. Increase in their thermal stability, oxidation and wear resistance is promoted by adding either metallic elements (Al, Zr, Ta, etc.) or nonmetallic elements such as Si or C. The incorporation of Si atoms into TiN, ZrN or CrN contributes to grain size refinement and the formation of a nanocomposite structure (grains of TM nitride surrounded by an amorphous SiNx phase), resulting in modification of mechanical properties together with enhanced thermal stability /2-4/. Unlike the Ti-Si-N system, the Zr-Si-N and Cr-Si-N films are less studied.

Preparation of thin films Nanocomposite ZrSiN films were grown by reactive magnetron sputter-deposition in a high vacuum chamber (base pressure < 10⁻⁵ Pa) equipped with three confocal targets configuration. Films were deposited on Si substrates covered with 10 nm thick thermally grown SiO₂ layer. A constant bias voltage of -60 V was applied to the substrate during deposition. Monolithic ZrN and Si₃N₄ films were also deposited as the reference films.

Water-cooled, 7.62-cm-diameter Zr (99.92 % purity), Si (99.995% purity, p-type doped) and Si₃N₄ (99.99 % purity) targets, located at 18 cm from the substrate holder, were used under Ar + N₂ plasma discharges at constant power mode. The Zr and Si target were operated in magnetically unbalanced configuration using a DC power supply, while a RF power supply was used for the Si₃N₄ target in balanced mode. The total working pressure was 0.21 Pa, as measured using a Baratron® capacitance gauge. The Ar/N₂ flow ratio was optimized to obtain stoichiometric nitrogen content in the films based on earlier results.

Nanocomposite ZrSiN films were deposited by co-sputtering from Zr and Si targets at the substrate temperature of 600 °C. The Si content in the films was varied by changing the DC power supply of the Si target, from 0 up to 200 W,

while maintaining the DC power supply of Zr targets constant. As a result, the coatings with Si content (CSi) ranging from 0 to 22.1 at.% were synthesized, as determined from elemental probe microanalysis. The total film thickness was ~ 300 nm.

Structure and phase composition of as-deposited nanocomposite ZrSiN films The analysis of ZrSiN films by TEM method allowed to conclude that their microstructure changes from nanocrystalline columnar grains ($0 \leq \text{CSi} \leq 3.2$ at.%) to a dual-phase structure characterized by the presence of grains included into a surrounding matrix ($\text{CSi} = 12.3$ at.% and $\text{CSi} = 17.2$ at.%) with increasing Si content. The cross-section TEM image for the case of $\text{CSi} = 12.3$ at.% is presented in Fig. 1a. The SAED pattern, shown in the insert, displays well-defined rings that can be indexed as 111, 200, 220 and 311 rings of a cubic (Na-Cl type) structure with a lattice parameter equal to 0.465 ± 0.005 nm, slightly higher than that of ZrN. When CSi increases up to 22.1 at. % the structure becomes close to amorphous (see Fig. 1b). However, the presence of diffuse rings indicates that short-range ordering is present for this sample (Fig. 1b, insert).

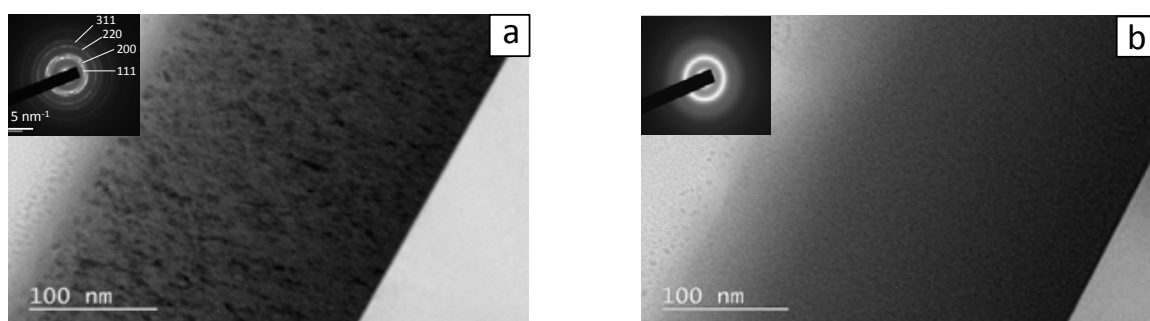


Fig. 1 - Cross-sectional bright field TEM micrographs of ZrSiN nanocomposite films with different silicon content: (a) $\text{CSi} = 12.3$ at.% and (b) $\text{CSi} = 22.1$ at.%. SAED patterns are shown in the insets.

Based on XPS data of the Si 2p emission lines for the ZrSiN films, the nature of the matrix which surrounds the ZrN grains in ZrSiN nanocomposite films with $\text{C}_{\text{Si}} \geq 12.3$ at.% was clarified. The Si 2p spectrum exhibits a main

peak centered at 101.85 eV, and a smaller one located near 98.4 eV. These two peaks can be assigned to Si 2p_{3/2} and Si 2p_{1/2} lines of amorphous silicon nitride (*a*-SiN_x) compound.

The results of XRD analysis for ZrN and ZrSiN films with different silicon content are given in Fig. 2 (see lower patterns corresponding to as-deposited state). The (111) preferred orientation prevails for ZrN reference film (Fig. 2a). When increasing C_{Si}, the strong decrease in 111 peak intensity and the concomitant increase in 200 peak intensity are observed (Fig. 2b,c). At the same time the broadening of peaks of zirconium nitride takes place. The crystallite size of ZrN phase decreases from 23 nm (ZrN film) down to 4-6 nm (ZrSiN film with 12.3 at.% \leq C_{Si} \leq 17.2 at.%) as it was extracted from XRD line broadening of 200 peak using Scherrer approximation. For ZrSiN film with C_{Si} = 22.1 at.% the size of the crystalline grains cannot any longer be estimated since it is X-ray amorphous.

From the obtained results, it is possible to infer about the formation of ZrSiN nanocomposite films representing bi-phase systems consisting of *a*-SiN_x amorphous matrix and cubic ZrN grains included into it.

Oxidation resistance of nanocomposite ZrSiN films under air annealing The appearance of crystalline oxide phases for ZrSiN nanocomposite films is revealed at higher temperatures in comparison with ZrN film (Fig. 2).

For ZrN film, the formation of tetragonal t-ZrO₂ oxide is already registered at the temperature of 550 °C (Fig. 2a). For ZrSiN nanocomposite films, the

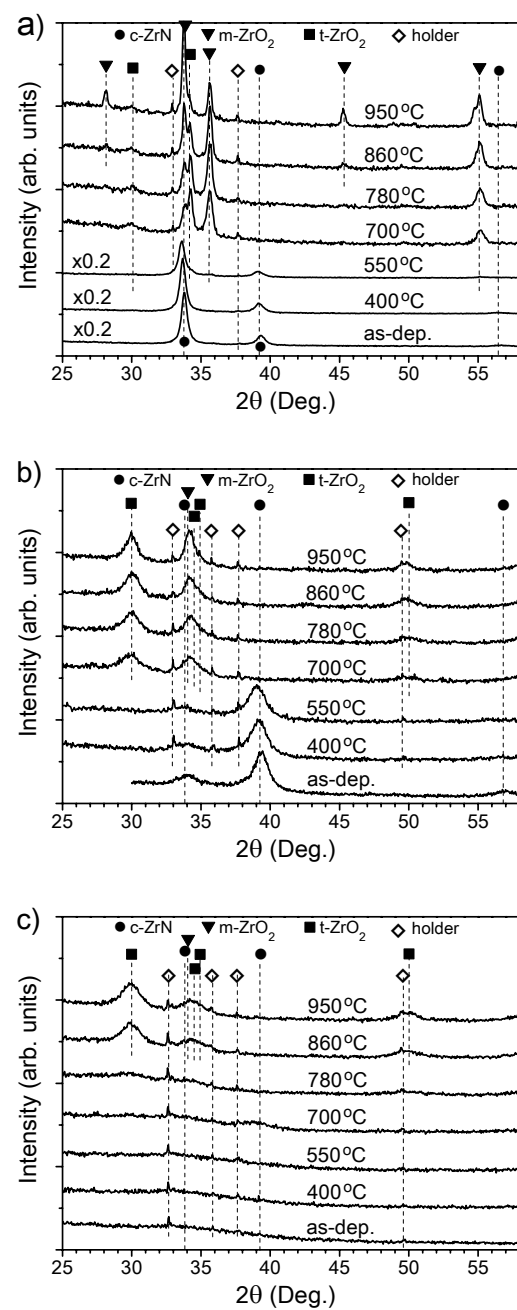


Fig. 2 - Evolution of XRD patterns under air annealing for ZrN reference film (a) and ZrSiN films with different silicon content: (b) C_{Si} = 12.3 at.% and (c) C_{Si} = 22.1 at.%.

oxidation starts at 700-780 °C (Fig. 2b-c). It should be mentioned that after annealing at the maximum temperature (950 °C) only t-ZrO₂ phase is revealed in ZrSiN films composition, unlike ZrN film where m-ZrO₂ phase is mainly present. The presence of the sole t-ZrO₂ phase for ZrSiN films could reflect that the oxidation process is not completed for these coatings, at least in the oxidation temperature and time ranges investigated here.

One can see for the ZrN reference film a high density of corrosion sites (Fig. 3), the presence of which leads to a coating swelling (Fig. 3a). The surface topography of the air-annealed Si₃N₄ coating exhibits extensive folded regions characteristic of blistering (Fig. 3b).

ZrSiN films retain a better surface integrity and there are no pronounced corrosion sites after air annealing at 950°C (Fig. 3c-d). However, these films tend to crack in consequence of constrained molar volume expansion associated with oxide formation during annealing.

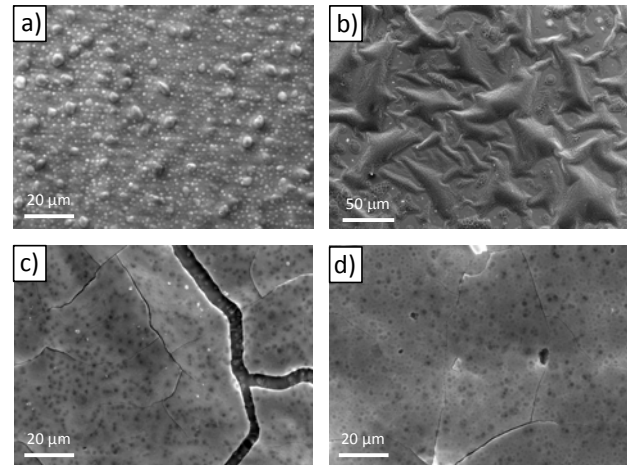


Fig. 3 - SEM micrographs of ZrN (a) and Si₃N₄ (b) reference films and ZrSiN nanocomposite films with C_{Si} = 12.3 at.% (c) and C_{Si} = 17.2 at.% (d) after air annealing at 950 °C.

Based on the obtained results one can conclude that with the increase of silicon content in ZrSiN films their resistance to high-temperature oxidation improves. However, after annealing at the maximum temperature of 950 °C, the cracking of these coatings occurs that interferes with retention of their protective properties.

Acknowledgments This work was supported by the project of Belarusian Republican Foundation for Fundamental Research (No. Ф18MC-027).

References

1. **Abadias G., et.al.** Thin Solid Films, 538 (2013) 56–70.
2. **Barshilia H.C., et.al.** Surf. Coat. Technol., 201 (2006) 329–337.
3. **Freitas F.G.R., et.al.** Materials Research, 18 (2015) 30–34.
4. **Lin J., et.al.** Surf. Coat. Technol., 216 (2013) 251–258.